

A Model-Based Sliding Mode Controller for Extensible Continuum Robots

APOORVA D. KAPADIA IAN D. WALKER DARREN M. DAWSON

Clemson University

Department of Electrical and Computer Engineering

105A Riggs Hall, Clemson, SC - 29634

USA

(akapadi,ianw,darren.dawson)@ces.clemson.edu

ENVER TATLICIOGLU

Izmir Institute of Technology

Department of Electrical & Electronics Engineering

Urla, Izmir 35430

Turkey

enver@envertatlicioglu.com

Abstract: In this paper, we present a new control strategy for continuous backbone (continuum) "trunk and tentacle" robots. Control of this emerging new class of robots has proved difficult due to the inherent complexity of their dynamics. Using a recently established full dynamic model, we introduce a new nonlinear model-based control strategy for continuum robots. The approach is applicable to continuum robots which can extend/contract as well as bend throughout their structure. Results are illustrated using a three-section, six degree of freedom planar continuum robot.

Key-Words: Sliding-Mode Control, Continuum Robot

1 Introduction

A continuum robot can be loosely defined as a robot with a continuously curving backbone [26] [32]. The unconventional morphology of continuum robots is largely the result of inspiration drawn from elements in the Animal Kingdom such as octopus arms, squid tentacles, and elephant trunks as seen in the prototypes and designs outlined in [11], [19] [22], [25], [27], and [31], among others. Continuum robots are most commonly used for whole arm grasping [1], navigation in unstructured environments [3], as well as manipulation of unstructured objects and payloads of various shapes and sizes [9].

Their unusual design allows continuum robots to work in congested environments and manipulate objects in spaces where traditional rigid-link robots with parallel-jaw grippers would otherwise be unsuccessful. While continuum manipulators have been deployed outside the laboratory environment [2], [12], given the sheer number of possible applications, most iterations have been surprisingly confined to a test environment. This is primarily due to the inability to model and compensate for the additional complexity inherent in the continuum structures of the numerous prototypes.

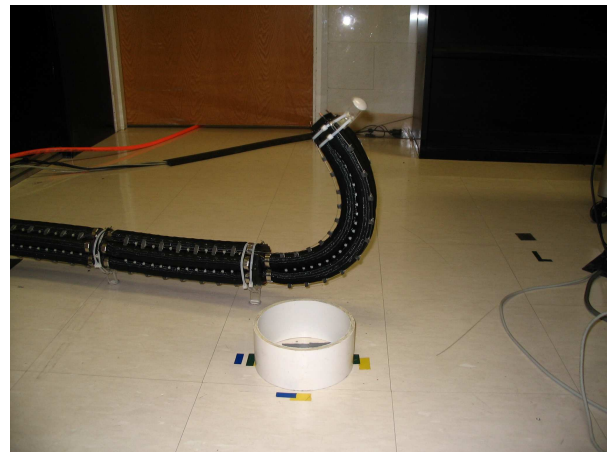


Figure 1: Octarm Bending

Thus, to better understand and utilize such manipulators, the development of sophisticated mathematical models is essential. Kinematic models for various types of continuum robots have been developed and proposed. Chirikjian and Burdick [5] developed kinematics for a general hyper-redundant manipulator which restricted the manipulator curve-shaping functions to a 'modal' form, allowing for quick computa-

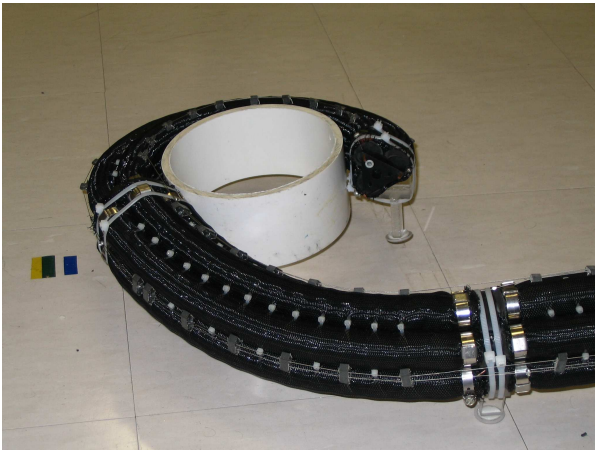


Figure 2: Octarm Whole Arm Grasping

tion of the inverse kinematic solution. This method is hindered in practice by the ability of manipulators to shape themselves as the curve-functions require. The authors of [4] developed kinematics based on similar previously-designed models for a pneumatically-driven kinematically redundant manipulator with a silicone rubber tip which could be used for colonoscopy. In [16], Jones and Walker extended early the kinematic developments in [10] for a general closed-form solution based on standard Denavit-Hartenberg techniques. The same authors added actuator length limits into the kinematic solutions derived previously [17], resulting in more practical, but complex shapes and solutions for continuum robot applications. Additionally, Gravagne and Walker developed kinematics using wavelet decomposition to derive novel kinematics for continuum robots [7] [8]. At this stage, kinematics for continuum robots is well understood.

Dynamic modeling for continuum manipulators has also been extensively analyzed. In [6], Chirikjian was one of the first to develop dynamics for a continuum robot, using an infinite degree of freedom model. In [18], the authors developed dynamics for an eel-like robot using a recursive version of the Newton-Euler equation and the Cosserat beam model, along with Navier-Stokes equations for fluid interaction in underwater environments. However, this model required zero initial accelerations regardless of the initial joint positions. Matsuni and Sato [23] developed a dynamic model for a snake-like robot having n -links. However while the model could be considered applicable to a hyper-redundant manipulator, the links were assumed to be rigid and thus the model was not appropriate for true continuous backbone continuum robots. Another dynamic model for a snake-like robot with rigid-links was proposed in [21]. Li *et al.* used the principles of virtual work to establish the



Figure 3: Octarm in Water

velocity and acceleration of the end-effector link and thus developed the forward and inverse kinematics, as well as the dynamic model. In [34], Yekutieli *et al.* developed a biological octopus arm dynamic model based on muscular hydrostats (a muscular hydrostat is the physiology that forms the structure of an octopus arm). However, the model is based on linear approximations and not appropriate for dynamics-based control development. Trivedi *et al.* [30] developed a non-closed-form, geometrically-exact dynamic model for soft robotic manipulators based on the theory of Cosserat rods, taking into account the large displacements and deformations due to material nonlinearities and distributed loads. More recent work [24], [28], and [29] has established closed-form Lagrangian dynamic models for continuum robots. That work forms the theoretical foundation for the work in this paper.

Having developed kinematic and dynamic models, the next step would be to apply them towards the development of model-based controllers to improve the performance of the hardware. The main focus of controller development is usually two fold; Obstacle avoidance, whole-arm grasping or similar joint-level control strategies, and/or end-effector position control in the task-space. Some of the first known controllers for continuum robots were proposed by Ivanescu *et al.* [13], [14], and [15]. In [14], the authors developed a highly specific set-point tracking variable structure controller for a tentacle arm whose physical model was based on composite materials consisting of electrorheostatic fluids. In [13], the authors developed an obstacle-avoidance controller based on the artificial potential field method with the goal of a desired final end effector position, using the dynamic model developed in [14]. In [15], the authors developed a sliding mode controller along with a fuzzy controller for two cooperating hyper-redundant robots. All these works were restricted to simulations.

In this paper, the development is strongly moti-

vated by improving the performance of the OCTARM (OCTopus ARM) [9], built by Pennsylvania State University and Clemson University, and closely resembling an Octopus arm or an Elephant trunk. As shown in Figure 4, the OCTARM is a 3 section manipulator having nine degrees-of-freedom; Each section can bend with constant curvature along two axes, as well as extend prismatically. The ability to extend as well as bend is significant. A key advantage of continuum robots over traditional rigid-link manipulators was highlighted by Walker *et al* in [33], showing the increased workspace afforded by the OCTARM due to its planar extension capabilities.

A basic non-model-based controller for the OCTARM was developed and implemented in [1], however, it was designed to compensate for the unknown dynamic model (subsequently, a kinematic model for the OCTARM was proposed in [17], while the Lagrangian dynamics for the Octarm were developed in [28] and [29]). None of the controllers described previously were found to be suitable for practical application on the Octarm, due to either the specific nature of the manipulator design, and thus the dynamic model, or the design of the controller. Performance was found to be either slow in response, subject to oscillatory motions, or both.

In this paper, we propose the application of a standard sliding mode controller developed for manipulators whose models are based on the Lagrangian dynamics, albeit with slight modifications so as to fit the structure of the Octarm's continuum dynamics. A Lyapunov-based stability proof is utilized for the stability analysis of the proposed controller, and numerical simulations are shown to highlight the effectiveness of the proposed controller in comparison to a standard dynamics-cancelling PD controller.

2 Control Development

2.1 Dynamic Model

In this paper, we build on a recently established [28], [29] continuum robot dynamic model formulation. The work in [28], [29] provides for the first time a closed form model, applicable to robot extension as well as bending, which contains key properties (well-established for conventional rigid-link robot structures) essential for nonlinear controller synthesis. In particular, the overall model takes the familiar form,

$$\tau(t) = M(q)\ddot{q} + N(q, \dot{q})\dot{q} + G(q) + B(q) + E(q), \quad (1)$$

where $q(t) \in \mathbb{R}^n$ is the variable joint position, $M(q)$ and $N(q, \dot{q}) \in \mathbb{R}^{n \times n}$ are the inertia and centripetal-coriolis matrices respectively. The terms $G(q)$, $B(q)$,

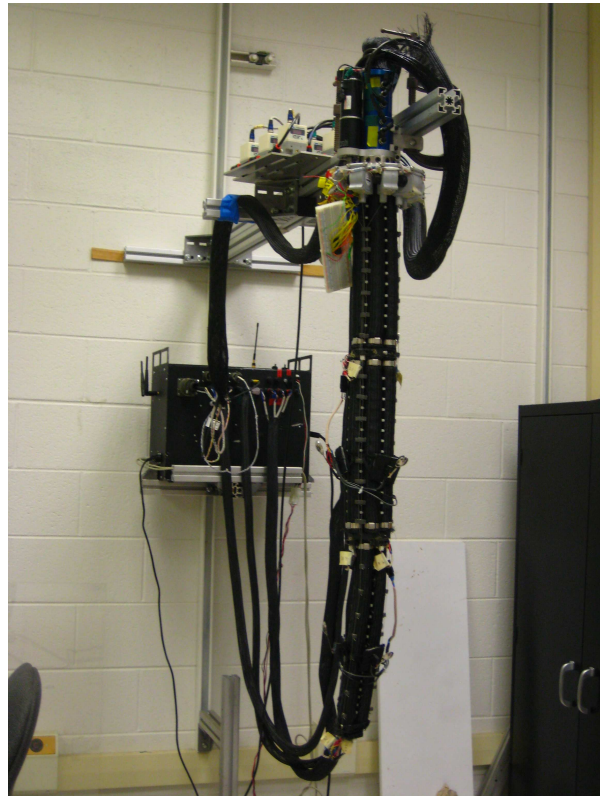


Figure 4: Octarm

and $E(q) \in \mathbb{R}^n$ represent the effects of gravitational energy, potential energy due to bending effects, and potential energy due to extension, respectively, and $\tau(t) \in \mathbb{R}^n$ is the control input. The model has the following properties,

1. The inertia matrix $M(q)$ is symmetric and positive definite.
2. The matrix $\dot{M} - 2V$ is skew-symmetric and satisfies the property

$$\xi^T (\dot{M} - 2N) \xi = 0 \quad \forall \xi \in \mathbb{R}^n \quad (2)$$

which we will exploit in the controller synthesis below.

2.2 Controller Synthesis

In the following, we use the dynamic model above to extend and adapt the nonlinear control approach in [20] to the case of extensible continuum robots. For simplicity, in the following, we assume planar motion of the Octarm in the plane perpendicular to gravity. In this case $G(q) = 0$, and $q(t) = [d_1, d_2, d_3, \kappa_1, \kappa_2, \kappa_3]$ (the extension lengths and bending curvatures for each of the three sections). The following analysis is,

however, general for full spatial motion and non-zero gravity.

Let the manipulator section tracking error, $e(t) \in \mathbb{R}^6$ be defined as,

$$e = q_d - q, \quad (3)$$

where $q_d(t) \in \mathbb{R}^6$ is the desired manipulator position. The first and second time derivatives of (3) are given by

$$\begin{aligned} \dot{e} &= \dot{q}_d - \dot{q} \\ \ddot{e} &= \ddot{q}_d - \ddot{q} \end{aligned} \quad (4)$$

in which $\dot{q}(t)$ and $\ddot{q}(t) \in \mathbb{R}^6$ represents the manipulator section velocity and acceleration respectively, and $\dot{q}_d(t)$ and $\ddot{q}_d(t) \in \mathbb{R}^6$ represents the desired manipulator section velocity and acceleration respectively. Let $r(t) \in \mathbb{R}^6$ be the sliding surface defined as the filtered tracking error such that

$$r = \alpha e + \dot{e} \quad (5)$$

where $\alpha = \text{diag}[\alpha_1, \alpha_2, \alpha_3, \alpha_4, \alpha_5, \alpha_6]$, in which $\alpha_i > 0$. Let $\dot{q}_r \in \mathbb{R}^6$ be the filtered trajectory given by

$$\dot{q}_r = \alpha e + \dot{q}_d. \quad (6)$$

Theorem 1 Consider the controller

$$\tau = \hat{M}\dot{q}_r + \hat{N} + \hat{G} + \hat{B} + \hat{E} + K \text{sgn}(r), \quad (7)$$

in which $\hat{M}(q) \in \mathbb{R}^{6 \times 6}$, $\hat{V}(q, \dot{q}) \in \mathbb{R}^{6 \times 6}$, $\hat{G}(q)$, $\hat{B}(q)$, and $\hat{E}(q) \in \mathbb{R}^6$ are the estimates of M , $V(q, \dot{q})$, $G(q)$, $B(q)$, and $E(q)$ respectively. Using this controller, the error reaches the sliding surface described in (5) in a finite time. In addition, once on the surface, $q(t)$ will go to $q_d(t)$ exponentially fast.

Proof: Consider a candidate Lyapunov function

$$V(r) = \frac{1}{2} r^T M(q) r \quad (8)$$

whose time derivative yields

$$\dot{V}(r) = r^T M \dot{r} + \frac{1}{2} \dot{M}(\dot{q}) r. \quad (9)$$

Substituting the time derivative of (5) in (9) and using the property of skew-symmetry of the model stated in Property 2 previously, results in

$$\dot{V}(r) = r^T [M\ddot{q}_r + N\dot{q}_r + G + B + E - \tau]. \quad (10)$$

Thus, using the controller given by (7), the following result is obtained

$$\dot{V}(r) = r^T \left[\tilde{M}\ddot{q}_r + \tilde{N}\dot{q}_r + \tilde{G} + \tilde{B} + \tilde{E} \right] - \sum_{i=1}^6 k_i |r_i|, \quad (11)$$

where $\tilde{M} = M - \hat{M}$, $\tilde{N} = N - \hat{N}$, $\tilde{G} = G - \hat{G}$, $\tilde{B} = B - \hat{B}$, $\tilde{E} = E - \hat{E}$. It is sufficient to choose $k_i \in \mathbb{R}$ such that

$$k_i \geq \left| \left[\tilde{M}\ddot{q}_r + \tilde{N}\dot{q}_r + \tilde{G} + \tilde{B} + \tilde{E} \right]_i \right| + \eta_i \quad (12)$$

where $\eta_i \in \mathbb{R} > 0$. Substituting (12) in (11) yields the following inequality

$$\dot{V}(r) \leq - \sum_{i=1}^6 \eta_i |r_i|, \quad (13)$$

from which it can be seen that $r(t) = 0$ is reached in finite time. Thus, from (5), when $r(t) = 0$, $\dot{e}(t) = 0$ and $e(t) = 0$ and once the system is in sliding mode, the tracking error $e(t)$ converges to zero exponentially fast. •

3 Controller Performance

To demonstrate the effectiveness of the control strategy introduced in the previous section, in this section we present the results of the controller applied to a simulation of the OCTARM manipulator. In the following, all three sections of the robot are actuated. For simplicity, the robot motions are restricted to the plane orthogonal to gravity. The robot thus has six degrees of freedom, three of extension/contraction (one for each link), and three for bending (again, one degree of bending freedom for each link).

In the simulation, the robot is modeled using the dynamic model of the previous section. The controller in the simulation has additive white Gaussian noise with $SNR = 60$ and *initial seed* = 30 introduced to simulate real-time errors due to modeling inaccuracies, sensor errors, time delays and other similar unaccounted-for dependencies. The nominal trajectories of the sections are an aggressive set of exponentially-damped sinusoids given by

$$q = \begin{bmatrix} 0.35 + 0.01 \sin(2\pi t) \\ 0.35 \\ 0.4 + 0.01 \sin(2\pi t) \\ 1 + 0.2 \sin(2\pi t) \\ 2 + 0.2 \sin(2\pi t) \\ 3 \end{bmatrix}, \quad (14)$$

and shown in Figures 5 and 6. The ability of the controller proposed in this paper to track the trajectories is compared with that of a conventional 'inverse dynamics' controller, i.e. PD controller with an inner linearization loop [20].

The results for the standard (PD) controller are illustrated in Figures 7, 8, 9, and 10 respectively. Note

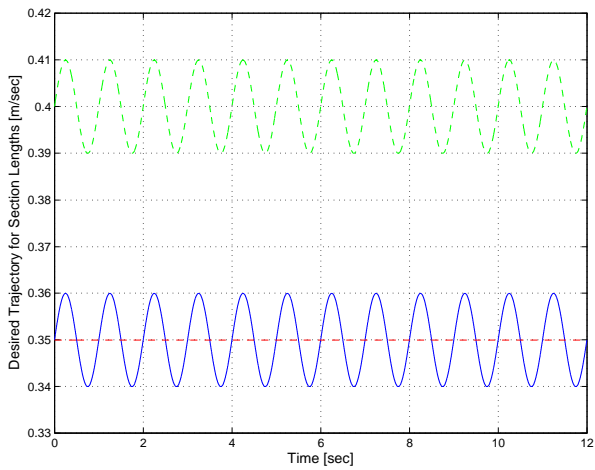


Figure 5: Desired Trajectories for the Lengths

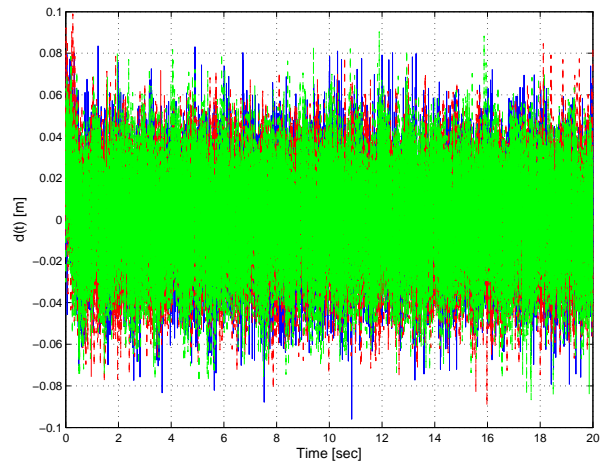


Figure 7: PD Controller Length Error

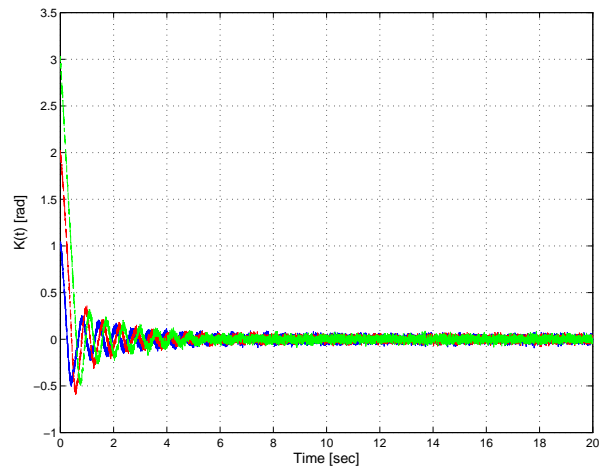


Figure 8: PD Controller Curve Error

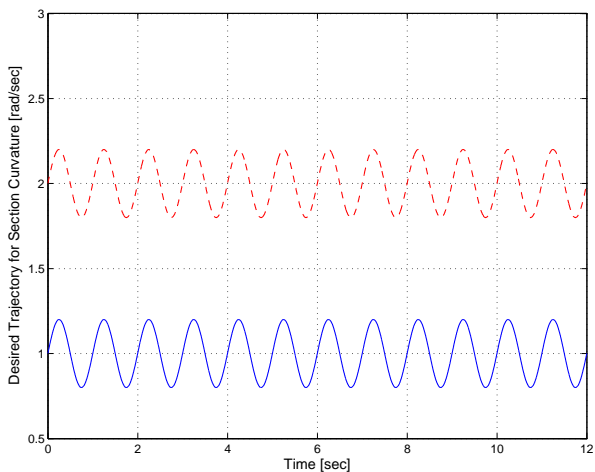


Figure 6: Desired Trajectories for the Curvatures

that the inverse dynamics controller includes all the possible problems and caveats associated with system inversion. This includes the possible presence of non-minimum phase zeros. Additionally, the gains required for optimal performance change depending on the nature of the performance objectives and also need to ensure that the system is critically damped.

The results for the controller introduced in (7) are illustrated in Figures 11, 12, 13, and 14 respectively. The hallmark of the sliding mode controller is that the error only needs to be driven to the a switching surface, after which the the system will not be affected by any modeling uncertainties or disturbances. Also, the additional caveats noted for the inverse dynamics controller do not apply in this case. A comparison of the plots in Figures 7, 8, 9, and 10 for the inverse dynamics PD controller, and Figures 11, 12, 13, and 14 reveal how the nonlinear controller successfully compensates for the dynamic uncertainty.

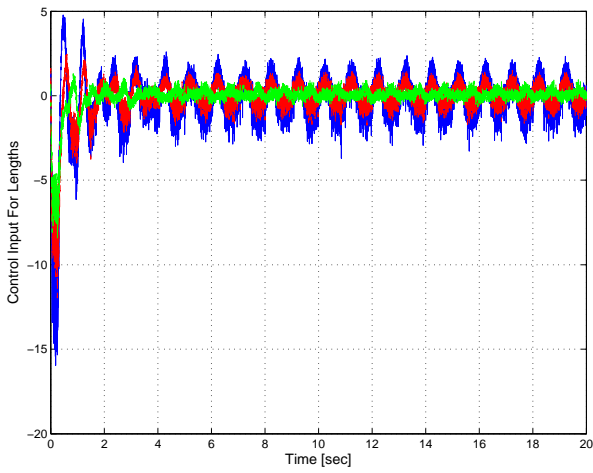


Figure 9: PD Controller Length Torque

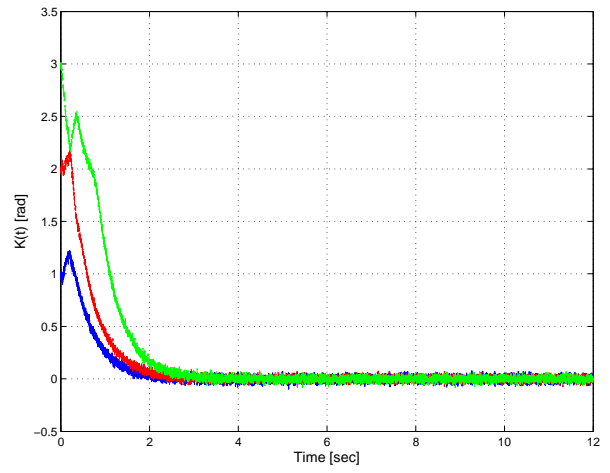


Figure 12: Sliding Mode Controller Curve Error

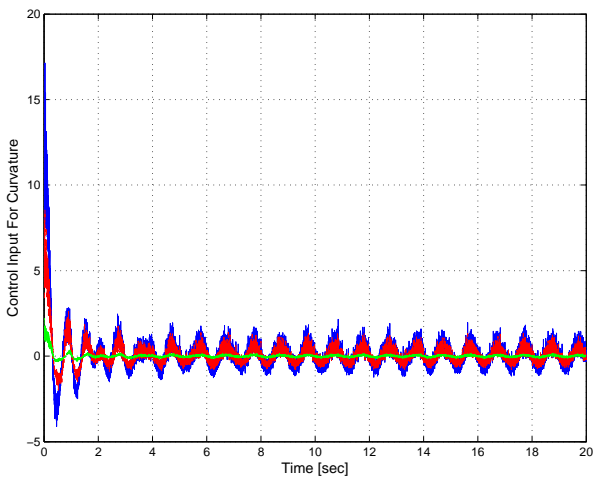


Figure 10: PD Controller Curve Torque

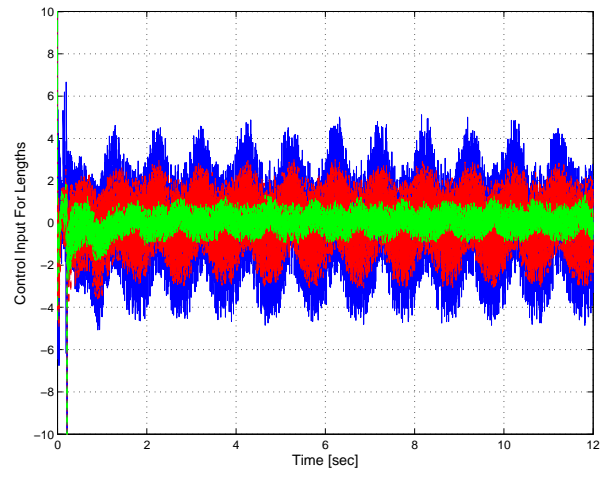


Figure 13: Sliding Mode Controller Length Torque

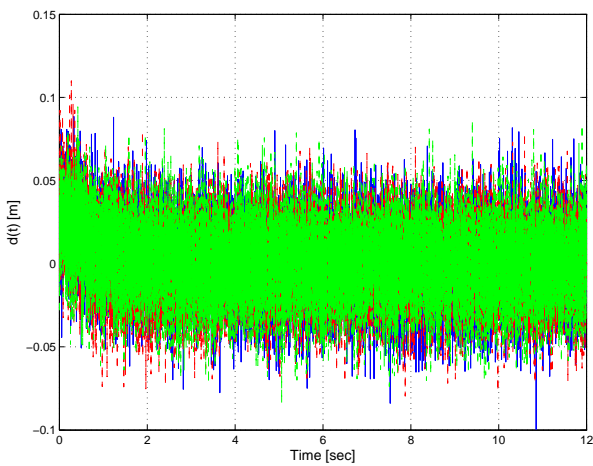


Figure 11: Sliding Mode Controller Length Error

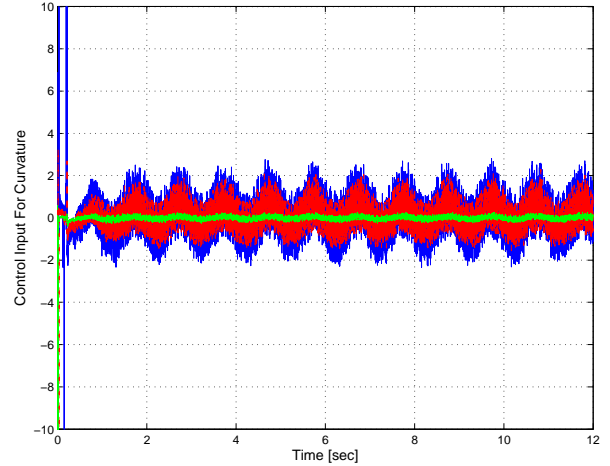


Figure 14: Sliding Mode Controller Curve Torque

4 Conclusions

We have presented a new model-based nonlinear controller for continuous backbone "continuum" robots. The model is based on a new formulation for continuum robot dynamics recently established in the literature. By exploiting the structure inherent in these dynamics, the controller is guaranteed to converge despite inherent errors due to uncertainty in model parameters. The results are applicable to continuum robots which extend as well as bend. Results of the controller are demonstrated via simulation of a three-section extensible continuum robot.

Acknowledgements: The research was supported

by the U.S. National Science Foundation under grants IIS-0844954 and IIS-0904116.

References:

- [1] D. Braganza, D.M. Dawson, I.D. Walker and N. Nath, A Neural Network Controller for Continuum Robots, *IEEE Trans. Robot.*, Vol. 23, No. 6, Dec. 2006, pp. 1270-1277.
- [2] R. Buckingham and A. Graham, Snaking Around in a Nuclear Jungle, *Ind. Robot: An Inter. Journ.*, Vol. 32 No. 2, Feb. 2005 pp. 120-127.
- [3] G. Chen, T. Pu, T. Herve and C. Prella, Design and Modeling of a Micro-Robotic Manipulator for Colonoscopy, *Proc. SICE Ann. Conf.*, Nancy, France, 2005 pp. 109-114.
- [4] G. Chen, M.T. Pham and T. Redarce, Development and kinematic analysis of a silicone-rubber bending tip for colonoscopy, *Proc. IEEE Int. Conf. Intell. Robo. Sys.*, Oct. 2006, pp. 168-173.
- [5] G.S. Chirikjian and J.W. Burdick, A Modal Approach to Hyper-Redundant Manipulator Kinematics, *IEEE Trans. Robot. Autom.*, Vol. 10, No. 3, Jun. 1994, pp. 343-354.
- [6] G.S. Chirikjian, Hyper-Redundant Manipulator Dynamics: A Continuum Approximation, *Adv. Robot.*, Vol. 9, No. 3, Jun. 1995, pp. 217-243.
- [7] I.A. Gravagne, and I.D. Walker, Kinematics for Constrained Continuum Robots Using Wavelet Decomposition, *Proc. Conf. and Expo. Robot. for Challenging Situ. and Environ.*, Albuquerque, NM, 2000, pp. 33-38.
- [8] I.A. Gravagne, and I.D. Walker, Kinematic Transformations for Remotely-Actuated Planar Continuum Robots, *Proc. IEEE Conf. Robot. Autom.*, San Francisco, CA, 2000, pp. 19-26.
- [9] M. Grissom, V. Chitrakaran, D. Dienno, M. Csencsits, M. Pritts, B. Jones, W. McMahan, D.M. Dawson, C. Rahn and I.D. Walker, Design and Experimental Testing of the OctArm Soft Robot Manipulator, *Proc. SPIE Conf. Unmanned Sys. Tech.*, Kissimmee, FL, 2006, pp. 109-114.
- [10] M.W. Hannan and I.D. Walker, Kinematics and the Implementation of an Elephants Trunk Manipulator and Other Continuum Style Robots, *J. Robot. Syst.*, Vol. 20, Feb. 2003, pp. 456-3.
- [11] S. Hirose, *Biologically Inspired Robots*, Oxford University Press, Oxford, U.K., 1993.
- [12] G. Immea and K. Antonelli, The KSI Tentacle Manipulator, *Proc. IEEE Int. Conf. Robot. Autom.*, Nagoya, Japan, 1995, pp. 3149-3154.
- [13] M. Ivansecu, N. Popescu and D. Popescu, A Variable Length Tentacle Manipulator Control System, *Proc. IEEE Int. Conf. Robot. Autom.*, Barcelona, Spain, 2005, pp. 3274-3279.
- [14] M. Ivansecu and V. Stoian, A Variable Structure Controller for a Tentacle Manipulator, *Proc. IEEE Int. Conf. Robot. Autom.*, Nagoya, Japan, 1995, pp. 3155-3160.
- [15] M. Ivansecu and V. Stoian, A Controller for Hyper-Redundant Cooperative Robots, *Proc. IEEE Int. Conf. Intel. Robot. Sys.*, Vancouver, Canada, 1998, pp. 167-172.
- [16] B. Jones and I.D. Walker, Kinematics for Multi-section Continuum Robots, *IEEE Trans. Robo.*, Vol. 22, No. 1, Feb. 2006, pp. 43-57.
- [17] B. Jones and I.D. Walker, Practical Kinematics for Real-Time Implementation of Continuum Robots, *IEEE Trans. Robo.*, Vol. 22, No. 6, Dec. 2006, pp. 1087-1099.
- [18] W. Khalil, G. Gallot, O. Ibrahim and F. Boyer, Dynamic Modeling of a 3-D Serial Eel-Like Robot, *Proc. IEEE Int. Conf. Robot. Autom.*, Barcelona, Spain, 2005, pp. 1282-1287.
- [19] D.M. Lane, B.C. Davies, G. Robinson, D.J. O'Brien, J. Sneddon, E. Seaton, and A. Elfstrom, The AMADEUS Dextrous Subsea Hand: Design, Modeling, and sensor processing, *IEEE Jour. Ocean. Eng.*, Vol. 24, No. 1, 1999, pp. 96-111.
- [20] F. Lewis, D.M. Dawson, and C. Abdallah *Robot Manipulator Control: Theory and Practice*, Marcell-Dekker Inc., New York, NY, 2004.
- [21] N. Li, T. Zhao and Y. Zhao, The Dynamic Modeling of Snake-Like Robot by Using Nominal Mechanism Method, *Intel. Robot. and Appl.*, Springer-Verlag, Berlin-Heidelberg 2008.
- [22] W. McMahan, B.A. Jones and I.D. Walker, Robotic Manipulators Inspired by Cephalopod Limbs, *Joun. Eng. Des. Inno.*, Vol. 1P, 2005, pp.01P2.

- [23] F. Matsuno and H. Sato, Trajectory Tracking of Snake Robots Based on Dynamic Model, *Proc. IEEE Int. Conf. Robot. Autom.*, Barcelona, Spain, 2005, pp. 3040-3045.
- [24] H. Mochiyama and T. Suzuki, Kinematics and Dynamics of a Cable-Like Hyper-Flexible Manipulator, *Proc. IEEE Int. Conf. Robot. Autom.*, Taipei, Taiwan, 2003, pp. 3672-3677.
- [25] H. Ohno and S. Hirose, Design of a Slim Slime Robot and its Gait of Locomotion, *Proc. IEEE Int. Conf. Intel. Robot. Sys.*, Maui, HI, 2001, pp. 707-715.
- [26] G. Robinson and J. Davies, Continuum Robots - A State of the Art, *Proc. IEEE Int. Conf. Robot. Autom.*, Detroit, MI, 1999, pp. 2849-2854.
- [27] K. Suzumori, S. Iikura and H. Tanaka, Development of a Flexible Microactuator and its Applications to Robotic Mechanisms, *Proc. IEEE Int. Conf. Robot. Autom.*, Sacramento, CA, 1991, pp. 1622-1627.
- [28] E. Tatlicioglu, I.D. Walker and D.M. Dawson, Dynamic Modeling for Planar Extensible Continuum Robot Manipulators, *Int. Jour. Robot. Autom.*, Vol. 24, No. 4, 2009, to appear.
- [29] E. Tatlicioglu, I.D. Walker and D.M. Dawson, New Dynamic Models for Planar Extensible Continuum Robot Manipulators, *IEEE Int. Conf. Intel. Robot. Sys.*, San Diego, CA, 2007, pp. 1485-1490.
- [30] D. Trivedi, A. Lofti and C.D. Rahn, Geometrically Exact Dynamic Models for Soft Robotic Manipulators, *IEEE Int. Conf. Intel. Robot. Sys.*, San Diego, CA, 2007, pp. 1497-1502.
- [31] H. Tsukagoshi, A. Kitagawa and M. Segawa, Active Hose: An Artificial Elephant's Nose with Maneuverability for Rescue Operations, *IEEE Int. Conf. Rob. Autom.*, Seoul, South Korea, 2001, pp. 2454-2459.
- [32] I.D. Walker, D.M. Dawson, T. Flash, F.W. Grasso, R.T. Hanlon, B. Hochner, W.M. Kier, C.F. Pagano, C.D. Rahn, Q.M. Zhang, Continuum Robot Arms Inspired by Cephalopods, *Proc. SPIE Conf. Unmanned Ground Veh. Tech. IV*, Orlando, FL, March 2005, pp. 303-314.
- [33] I.D. Walker, C. Carreras, R. McDonnell and G. Grimes, Extension versus Bending for Continuum Robots, *Int. Jour. Adv. Robot. Sys.*, Vol. 3, No. 2, Jun. 2006, pp. 303-314. pp. 171-178.
- [34] Y. Yekutieli, R. Sagiv-Zohar, R. Aharonov, Y. Engel, B. Hochner and T. Flash, Dynamic Model of the Octopus Arm I. Biomechanics of the Octopus Arm Reaching Movement, *Journ. Neurophy.*, Vol. 94, 2005, pp. 1443-1458. pp. 187-195.